# An exact Riemann solver for one-dimensional multi-material elastic-plastic flows with Mie-Grüneisen equation of state

Li Liu[1], Jun-bo Cheng [1,*], Jiequan Li [1]

June 4, 2019

**Abstract**

A multi-material HLLC-type approximate Riemann solver with both elastic and plastic waves (MHLLCEP) is constructed for 1D elastic-plastic flows with the hypo-elastic model and the von Mises yielding condition. Although Cheng in 2016 introduced a HLLC Riemann solver with elastic waves(HLLCE) for 1D elastic-plastic flows, Cheng assumed that pressure is continuous across the contact wave. This assumption maybe lead to big errors, especially for multi-material elastic-plastic flows. In our MHLLCEP, this assumption is not used again, and correspondingly the errors introduced by the assumption are deleted, describing and evaluating the plastic waves are more accurate than that in the HLLCE. Moreover, if the non-linear waves in the Riemann problem are only shock waves, even with the plastic waves, our MHLLCEP is theoretically accurate. For the multi-material system, in this paper, a ghost cell method is used to achieve a high-order spatial reconstruction across the interface without numerical oscillations. Based on the MHLLCEP, combining with the third-order WENO reconstruction method and the third-order Runge-Kutta method in time, a high-order cell-centered Lagrangian scheme for 1D multi-material elastic-plastic flows is built in this paper. A number of numerical experiments are carried out. Numerical results show that the presented third-order scheme is convergent, robust, and essentially non-oscillatory. Moreover, for multi-material elastic-plastic flows, the scheme with the MHLLCEP is more accurate and reasonable in resolving the multi-material interface than the scheme with the HLLCE.

## 1 Introduction

In this paper, an exact Riemann solver is built for one-dimensional multi-material elastic-plastic flows with the Mie-Grüneisen EOS, hypo-elastic constitutive model [1] and the von Mises' yielding condition.

The elastic-plastic flow is used to describe the deformation process of solid materials under strong dynamics loading, such as explosive or high-speed impact. The simulation of elastic-plastic flows has important application backgrounds, especially in the Implosion Dynamics weapon and Inertial Confine Fusion (ICF). The first try of simulating the elastic-plastic flows was given by Wilkins [1] in 1960s.

In the development history of hydrodynamic numerical methods, the exact Riemann solver has played a very important role as it not only can give a guide and reference to the construction of approximate Riemann solvers, but also can be used to determine the convergence and stability of numerical schemes. However, building the exact Riemann solver for 1D elastic-plastic flows is not that easy. Comparing with the governing equations system of 1D pure fluids, for 1D elastic-plastic flows, there are two more equations: a non-conservative constitutive equation and the von Mises yielding condition. The non-conservative character of the constitutive equation increases the difficulty in constructing Riemann solvers, while the von Mises yielding condition may leads to more non-linear waves in the structure of Riemann solvers. Moreover, in a general way, the equation of state(EOS) for solid materials is more complex than that for pure fluids, which directly increases the difficulty in solving the Riemann problem.

For the elastic-plastic flow with the hypo-elastic constitutive model and the von Mises' yielding condition, some approximate Riemann solvers[2, 3, 4, 5] have been developed recently. However, for the exact Riemann solver, the research is relatively few, and them are only considered with simple constitutive models and simple EOSs. For example, Garaizar [6] and Miller [7] introduced an exact Riemann solver for elastic or hyper-elastic materials, Gao and Liu [8, 9] firstly considered the yielding effect and developed an exact elastic-perfectly plastic solid Riemann solver, but the EOS used by them is very simple: in the elastic state, the material derivative of pressure is the linear function of the strain rate, which means the energy equation is not necessary; in the plastic state, a linear "stiffened-gas" EOS was used. All these makes easily deduce the relation across a non-linear wave. Although there are many cases considered in their works [8, 9], for every case, they can easily obtain the exact solution. But for many engineering problems, the EOS is more complex, and the energy equation has to be included during simulating. For these engineering solid problems with a complex constitutive and a complex EOS, such as the Mie-Grüneisen EOS, up to now, there is no exact Riemann solution.

In this paper, we want to construct an exact Riemann solver for the system of 1D elastic-plastic flows with the Mie-Grüneisen EOS, the hypo-elastic constitutive model and the von Mises' yielding condition. As every knows, the Mie-Grüneisen EOS is complex and is used widely in many engineering problems, which makes the energy equation must be included in the system of elastic-plastic flows and so we have to use some special methods to resolve the rarefaction wave. Otherwise, we analyse the Jacobian matrix and find, in the wave structures of Riemann solvers, there may be three to five waves, including one contact wave and other two to four non-linear waves. These nonlinear waves may be elastic shock waves, elastic rarefaction waves, plastic shock waves or plastic rarefaction waves. Moreover, elastic wave runs always faster than the followed plastic wave. So there are thirty-six possible cases of the wave structures in the Riemann solver.

This paper is organized as follows. In section 2, we introduce the governing equations to be studied. In section 3, the Riemann problem and the relations for every wave type (contact wave, shock wave and rarefaction wave) are derived. Then, the exact Riemann solver is given in section 4. The half Riemann problem and its solver is introduced in section 5. Some numerical examples are presented to validate the method in section 6. Conclusions are shown in section 7.

# 2 Governing equations

In this paper, the elastic energy is not included in the total energy. The exclution of the elastic energy is usual for practical engineering problems [10] and is different from that in Ref.[2].

## 2.1 Motion equations

For a continuous one-dimensional homogeneous solid, the motion equations in differential form are

$$\partial_t \mathbf{U} + \partial_x \boldsymbol{F}(\mathbf{U}) = 0,\ x \in\ \Omega \subset \mathbf{R},\ t > 0,$$

where

$$\mathbf{U} = \begin{bmatrix} \rho \\ \rho u \\ \rho E \end{bmatrix}, \quad \mathbf{F} = \begin{bmatrix} \rho u \\ \rho u^2 - \sigma \\ (\rho E - \sigma) u \end{bmatrix}, \tag{2.1}$$

$\rho$, $u$, $\sigma$ and $E$ are the density, velocity in $x-$direction, Cauchy stress and total energy per unit volume, respectively, $E$ has the relation with specific internal energy $e$ as

$$E = e + \frac{1}{2} u^2, \tag{2.2}$$

$$\sigma = -p + s_{xx}, \tag{2.3}$$

where $p$ and $s_{xx}$ denote hydrostatic pressure and deviatoric stress in the $x-$ direction, respectively.

## 2.2 The equation of state (EOS)

The relation of the pressure with the density and the specific internal energy is gotten from the equation of state (EOS). In this paper, we consider the Mie-Grüneisen EOS,

$$p(\rho, e) = \rho_0 a_0^2 f(\eta) + \rho_0 \Gamma_0 e, \tag{2.4}$$

where $f(\eta) = \frac{(\eta-1)(\eta-\Gamma_0(\eta-1)/2)}{(\eta-s(\eta-1))^2}$, $\eta = \frac{\rho}{\rho_0}$, $\rho_0$, $a_0$, $s$ and $\Gamma_0$ are constant parameters of the Mie-Grüneisen EOS.

## 2.3 The constitutive relation

Hooke's law is used here to describe the relationship between the deviatoric stress and the strain,

$$\dot{s}_{xx} = 2\mu\left(\dot{\varepsilon}_x - \frac{1}{3}\frac{\dot{V}}{V}\right), \tag{2.5}$$

where $\mu$ is the shear modulus, $V$ is the volume, and the dot means the material time derivative,

$$\dot{()} = \frac{\partial()}{\partial t} + u\frac{\partial()}{\partial t}, \tag{2.6}$$

and

$$\dot{\varepsilon}_x = \frac{\partial u}{\partial x}, \quad \frac{\dot{V}}{V} = \frac{\partial u}{\partial x}. \tag{2.7}$$

By using Eq.(2.7), Eq.(2.5) can be rewritten as

$$\frac{\partial s_{xx}}{\partial t} + u\frac{\partial s_{xx}}{\partial t} = \frac{4}{3}\mu\frac{\partial u}{\partial x}. \tag{2.8}$$

## 2.4 The yielding condition

The Von Mises' yielding condition is used here to describe the elastic limit. In one spatial dimension, the von Mises' yielding criterion is given by

$$|s_{xx}| \leq \frac{2}{3}Y_0, \tag{2.9}$$

where $Y_0$ is the yield strength of the material in simple tension.

# 3 The Riemann problem

The Riemann problem for the 1D time dependent elastic-plastic equations is given as follows:

$$\begin{cases} \partial_t\rho + \partial_x(\rho u) = 0, \\ \partial_t(\rho u) + \partial_x(\rho u^2 + p - s_{xx}) = 0, \\ \partial_t(\rho E) + \partial_x\left[(\rho E + p - s_{xx})u\right] = 0, \\ \partial_t s_{xx} + u\partial_x s_{xx} - \dfrac{4}{3}\partial_x u = 0, \\ |s_{xx}| \leq \dfrac{2}{3}Y_0, \\ Q(x, t=0) = \begin{cases} Q_L, & \text{if } x < 0, \\ Q_R, & \text{if } x \geq 0, \end{cases} \end{cases} \tag{3.1}$$

where $Q = (\rho, \rho u, \rho E, s_{xx})^T$.

The above equations are just for the elastic status of the solid material. If the material are in the plastic state, the above equations can be simplified and correspondingly the jacobian matrix and sonic velocity are different. We will discuss them separately.

## 3.1 Elastic state

### 3.1.1 Jacobian matrix in elastic regions

For the Mie-Grüneisen EOS, if the material is not yielding,

$$|s_{xx}| < \frac{2}{3}Y_0, \tag{3.2}$$

the system (3.1) can be written as

$$\partial_t \mathbf{Q} + \mathbf{J}_e(\mathbf{Q})\partial_x \mathbf{Q} = 0, \tag{3.3}$$

where $Q = (\rho, \rho u, \rho E, s_{xx})$, and the Jacobian matrix is

$$\mathbf{J}_e(Q) = \begin{bmatrix} 0 & 1 & 0 & 0 \\ -u^2 + \frac{\partial p}{\partial \rho} + \Gamma(\frac{u^2}{2} - e) & u(2-\Gamma) & \Gamma & -1 \\ (\Gamma(\frac{u^2}{2} - e) - e - \frac{u^2}{2} + \frac{\sigma}{\rho} + \frac{\partial p}{\partial \rho})u & -\Gamma u^2 - \frac{\sigma}{\rho} + \frac{u^2}{2} + e & (1+\Gamma)u & -u \\ \frac{4}{3}\mu\frac{u}{\rho} & -\frac{4}{3}\mu\frac{1}{\rho} & 0 & u \end{bmatrix}, \tag{3.4}$$

where $\Gamma = \frac{\Gamma_0 \rho_0}{\rho}$.

The eigenvalues of $\mathbf{J}_e(\mathbf{Q})$ are given as

$$\lambda_1 = \lambda_2 = u, \quad \lambda_3 = u - c_e, \quad \lambda_4 = u + c_e, \tag{3.5}$$

where $c_e$ means the sonic speed of the solid in the elastic state,

$$\begin{cases} c_e = \sqrt{a^2 - \dfrac{\rho_0}{\rho^2}\Gamma_0 s_{xx} + \dfrac{4}{3}\dfrac{\mu}{\rho}}, \\ a^2 = \dfrac{\partial p}{\partial \rho} + \dfrac{p}{\rho^2}\dfrac{\partial p}{\partial e} = a_0^2 \dfrac{\partial f}{\partial \eta} + \dfrac{p}{\rho^2}\rho_0\Gamma_0. \end{cases} \tag{3.6}$$

The corresponding right eigenvectors are

$$r_1 = \begin{bmatrix} \frac{1}{b_1} \\ \frac{u}{b_1} \\ 0 \\ 1 \end{bmatrix}, \quad r_2 = \begin{bmatrix} -\frac{\Gamma}{b_1} \\ -\frac{\Gamma u}{b_1} \\ 1 \\ 0 \end{bmatrix}, \quad r_3 = \frac{1}{\phi^2}\begin{bmatrix} 1 \\ u - c_e \\ h - uc_e \\ \phi^2 \end{bmatrix}, \quad r_4 = \frac{1}{\phi^2}\begin{bmatrix} 1 \\ u + c_e \\ h + uc_e \\ \phi^2 \end{bmatrix}, \tag{3.7}$$

where

$$b_1 = \frac{\partial p}{\partial \rho} - \Gamma E, \quad h = E + \frac{p - s_{xx}}{\rho}, \tag{3.8}$$

and

$$\phi^2 = a^2 - \frac{\rho_0}{\rho^2}\Gamma_0 s_{xx} - c_e^2 = -\frac{4\mu}{3}\frac{1}{\rho}. \tag{3.9}$$

### 3.1.2 A relation between $\rho$ and $s_{xx}$

Thanks to (2.6), the equations of the density and the deviatoric stress in Eq.(3.1) can be written as

$$\frac{\partial u}{\partial x} = -\frac{1}{\rho}\frac{d\rho}{dt}, \tag{3.10}$$

and

$$\frac{ds_{xx}}{dt} = \frac{4}{3}\mu\frac{\partial u}{\partial x}. \tag{3.11}$$

Substituting (3.10) into (3.11) yields

$$\frac{ds_{xx}}{dt} = -\frac{4}{3}\mu\frac{1}{\rho}\frac{d\rho}{dt}. \tag{3.12}$$

Integrate the above equation from the data in front of a wave to the data behind the wave and perform some simple algebraic manipulations, one can get

$$s_{xx} + \frac{4}{3}\mu \ln(\rho) = \text{constant} \tag{3.13}$$

This relation always hold in the elastic state.

### 3.1.3 Relations across the contact wave

For a system without molecular diffusion, there is no materials convecting across the contact wave or interface, so the velocities on two sides of the discontinuity are always equal. This can also be verified by the eigenvectors in Eq.(3.7) and Eq.(3.62).

Using $\mathbf{Q}_L^*$ and $\mathbf{Q}_R^*$ to denote the two data states connected the contact wave, where $\mathbf{Q} = (\rho, u, p, s_{xx})$.

Thanks to Eq.(3.7), for the $\lambda_1$-wave we have

$$\frac{d\rho}{\frac{1}{b_1}} = \frac{d\rho u}{\frac{u}{b_1}} = \frac{d\rho E}{0} = \frac{ds_{xx}}{1}. \tag{3.14}$$

From the above equations, we can easily deduce that

$$du = 0, \quad d(s_{xx} - p) = 0, \tag{3.15}$$

which means

$$u_L^* = u_R^*, \tag{3.16}$$

and

$$\sigma_{x,L}^* = \sigma_{x,R}^*, \tag{3.17}$$

where $()_L^*$ and $()_R^*$ denote $()$ in the region of $\mathbf{Q}_L^*$ and $\mathbf{Q}_R^*$, respectively. Here we do not show the details of the derivation for a simple presentation.

Similarly, for the $\lambda_2$-wave one has

$$\frac{d\rho}{\frac{-\Gamma}{b_1}} = \frac{d\rho u}{\frac{-u\Gamma}{b_1}} = \frac{d\rho E}{1} = \frac{ds_{xx}}{0}. \tag{3.18}$$

From the above equations, we can easily deduce that

$$du = 0, \quad dp = 0, \quad ds_{xx} = 0, \tag{3.19}$$

which means

$$u_L^* = u_R^*, \tag{3.20}$$

$$p_L^* = p_R^*, \quad s_{xx,L}^* = s_{xx,R}^*. \tag{3.21}$$

From Eq.(3.21), we get that

$$\sigma_{x,L}^* = \sigma_{x,R}^*. \tag{3.22}$$

At last, for the $\lambda_1$ and $\lambda_2$ waves, one can find that the following two relations always hold:

$$u_L^* = u_R^*, \quad \sigma_{x,L}^* = \sigma_{x,R}^*. \tag{3.23}$$

For convenience, we define

$$s^* = u_L^* = u_R^*. \tag{3.24}$$

where $s^*$ denotes the velocity of the contact wave.

### 3.1.4 Relations across rarefaction waves

***Left-going rarefaction wave*** Across the left wave associated with $\lambda_3$-wave, ($\lambda_3 = u - c_e$), we have

$$\frac{d\rho}{1} = \frac{d(\rho u)}{u - c_e} = \frac{d(\rho E)}{h - uc_e} = \frac{ds_{xx}}{-\frac{4\mu}{3}\frac{1}{\rho}}. \tag{3.25}$$

which leads to

$$\mathrm{d}u = -\frac{c_e}{\rho}\mathrm{d}\rho, \tag{3.26}$$

$$\mathrm{d}E = -\frac{\sigma + \rho u c_e}{\rho^2} d\rho, \tag{3.27}$$

$$\mathrm{d}s_{xx} = -\frac{4}{3}\frac{\mu}{\rho} d\rho. \tag{3.28}$$

Using (2.4), one can get

$$dE = de + udu. \tag{3.29}$$

Substituting (3.26) and (3.27) into the above equation yields

$$de = -\frac{\sigma}{\rho^2}d\rho = \frac{p - s_{xx}}{\rho^2}d\rho. \tag{3.30}$$

Thanks to (2.4), one can get

$$dp = \frac{\partial p}{\partial \rho}d\rho + \frac{\partial p}{\partial e}de = a_0^2\frac{\partial f}{\partial \eta}d\rho + \rho_0\Gamma_0 de, \tag{3.31}$$

Substituting (3.30) into the above equation yields

$$dp = \left(a_0^2\frac{\partial f}{\partial \eta} + \frac{p}{\rho^2}\rho_0\Gamma_0 - \frac{\rho_0}{\rho^2}\Gamma_0 s_{xx}\right)d\rho. \tag{3.32}$$

The above equation can be rewritten as a differential equation of $p(\rho)$

$$p'(\rho) - \lambda\frac{p}{\rho^2} = f_2(\rho), \tag{3.33}$$

where

$$\lambda = \rho_0\Gamma_0 \quad f_2(\rho) = a_0^2\frac{\partial f}{\partial \eta} - \lambda\frac{s_{xx}(\rho)}{\rho^2}. \tag{3.34}$$

By integrating (3.33) across the left rarefaction wave, the pressure can be solved out as

$$pe^{\frac{\lambda}{\rho}} - \int f_2(\rho)e^{\frac{\lambda}{\rho}}d\rho = \text{constant}. \tag{3.35}$$

Integrating (3.26) across the left rarefaction wave yields

$$u + \int \frac{c_e}{\rho}d\rho = \text{constant}. \tag{3.36}$$

***Right-going rarefaction wave***

Across the right wave associated with $\lambda_4$-wave, ($\lambda_3 = u + c_e$), we have

$$\frac{d\rho}{1} = \frac{d(\rho u)}{u + c_e} = \frac{d(\rho E)}{h + uc_e} = \frac{ds_{xx}}{-\frac{4\mu}{3}\frac{1}{\rho}}. \tag{3.37}$$

which leads to

$$\mathrm{d}u = \frac{c_e}{\rho}\mathrm{d}\rho, \tag{3.38}$$

$$\mathrm{d}E = -\frac{\sigma + \rho u c_e}{\rho^2}\mathrm{d}\rho, \tag{3.39}$$

$$\mathrm{d}s_{xx} = -\frac{4}{3}\frac{\mu}{\rho}\mathrm{d}\rho. \tag{3.40}$$

By using the same method, one can get

$$pe^{\frac{\lambda}{\rho}} - \int f_2(\rho)e^{\frac{\lambda}{\rho}}d\rho = \text{constant}. \tag{3.41}$$

$$u - \int \frac{c_e}{\rho}d\rho = \text{constant}. \tag{3.42}$$

### 3.1.5 Relations across shock waves

Now we consider a shock wave moving with the speed of $s$. The data in front of the shock is $(\rho_1, u_1, p_1, s_{xx1})$ and that after the shock is $(\rho_2, u_2, p_2, s_{xx2})$.

We transform the equations to a frame of reference moving with the shock and the Rankine-Hugoniot Conditions give

$$\rho_2(u_2 - s) = \rho_1(u_1 - s), \tag{3.43}$$

$$\rho_2 u_2(u_2 - s) = \rho_1 u_1(u_1 - s) + \sigma_2 - \sigma_1, \tag{3.44}$$

$$\rho_2 E_2(u_2 - s) = \rho_1 E_1(u_1 - s) + \sigma_2 u_2 - \sigma_1 u_1. \tag{3.45}$$

Substituting (3.43) into (3.44) yields

$$\rho_1(u_2 - u_1)(u_1 - s) = \sigma_2 - \sigma_1. \tag{3.46}$$

From (3.43), one has

$$u_1 - s = \frac{(u_1 - u_2)\rho_2}{\rho_2 - \rho_1}, \tag{3.47}$$

then subtituting it into (3.46) yields

$$-t(u_2 - u_1)^2 = \sigma_2 - \sigma_1, \tag{3.48}$$

where $t = \frac{\rho_1\rho_2}{\rho_2 - \rho_1}$.

By using the same methods for (3.45), (3.45) can be written as

$$t(u_1 - u_2)(E_2 - E_1) = \sigma_2 u_2 - \sigma_1 u_1. \tag{3.49}$$

Because of $E = e + \frac{1}{2}u^2$, we can get

$$e_2 - e_1 = -\frac{\sigma_1 + \sigma_2}{2t}. \tag{3.50}$$

Using the EOS of Mie-Grüneisen (2.4), can get

$$e = c_0 p - c_1 f(\rho/\rho_0), \tag{3.51}$$

where $c_0 = \frac{1}{\rho_0\Gamma_0}$ and $c_1 = \frac{a_0^2}{\Gamma_0}$. Put the above equation into (3.50), we can solve the pressure $p_2$ out as a function of $\rho_2$.

$$p_2 = \frac{2t(c_1 f(\rho_2/\rho_0) + e_1) - (\sigma_1 + s_{xx2})}{2tc_0 - 1}. \tag{3.52}$$

Thanks to (3.13), $s_{xx2}$ can be written as

$$s_{xx2} = s_{xx1} - \frac{4}{3}\mu\ln(\frac{\rho_2}{\rho_1}). \tag{3.53}$$

Then, the Cauchy stress can be written as

$$\sigma_2 = -p_2 + s_{xx2}. \tag{3.54}$$

Then we can use (3.48) to solve the velocity after the shock

$$u_2 = \begin{cases} u_1 - \sqrt{\dfrac{\sigma_1 - \sigma_2}{t}} & \text{Left-going,} \\ u_1 + \sqrt{\dfrac{\sigma_1 - \sigma_2}{t}} & \text{Right-going.} \end{cases} \tag{3.55}$$

And the shock speed is given as

$$s = \frac{\rho_2 u_2 - \rho_1 u_1}{\rho_2 - \rho_1}. \tag{3.56}$$

By the above deductions for the moving shock wave, we can find that, if the density after the shock is known, all the data after the shock can be solved out.

## 3.2 Plastic state

When the material is yielding,

$$|s_{xx}| = \frac{2}{3}Y_0, \tag{3.57}$$

the equations of Riemann problem will turn into a more simple system with only constitutive terms as

$$\begin{cases} \partial_t\rho + \partial_x(\rho u) = 0, \\ \partial_t(\rho u) + \partial_x(\rho u^2 + p - s_{xx}) = 0, \\ \partial_t(\rho E) + \partial_x\left[(\rho E + p - s_{xx})u\right] = 0, \\ |s_{xx}| = \dfrac{2}{3}Y_0, \\ U(x, t=0) = \begin{cases} U_L, & \text{if } x < 0, \\ U_R, & \text{if } x \geq 0, \end{cases} \end{cases} \tag{3.58}$$

where $\mathbf{U} = (\rho, \rho u, \rho E)$.

### 3.2.1 Jacobian matrix in plastic regions[1]

The equations (3.58) can be written as

$$\partial_t\mathbf{U} + \mathbf{J}_p(\mathbf{U})\partial_x\mathbf{U} = 0, \tag{3.59}$$

where the Jacobian matrix is

$$\mathbf{J}_p(\mathbf{U}) = \begin{bmatrix} 0 & 1 & 0 \\ -u^2 + \frac{\partial p}{\partial \rho} + \Gamma(\frac{u^2}{2} - e) & u(2-\Gamma) & \Gamma \\ (\Gamma(\frac{u^2}{2} - e) - e - \frac{u^2}{2} + \frac{\sigma}{\rho} + \frac{\partial p}{\partial \rho})u + \frac{u^2}{2} & -\Gamma u^2 - \frac{\sigma}{\rho} + e & (1+\Gamma)u \end{bmatrix}. \tag{3.60}$$

The eigenvalues of the coefficient matrix $\mathbf{J}_p(\mathbf{Q})$ are given as

$$\lambda_1 = u, \quad \lambda_2 = u - c, \quad \lambda_3 = u + c,$$

where

$$\begin{cases} c_p = \sqrt{a^2 - \dfrac{\rho_0}{\rho^2}\Gamma_0 s_{xx}}, \\ a^2 = \dfrac{\partial p}{\partial \rho} + \dfrac{p}{\rho^2}\dfrac{\partial p}{\partial e} = a_0^2\dfrac{\partial f}{\partial \eta} + \dfrac{p}{\rho^2}\rho_0\Gamma_0. \end{cases} \tag{3.61}$$

The corresponding right eigenvectors are

$$r_1 = \begin{bmatrix} -\frac{\Gamma}{b_1} \\ -\frac{\Gamma u}{b_1} \\ 1 \end{bmatrix}, \quad r_2 = \frac{1}{h - uc_p}\begin{bmatrix} 1 \\ u - c_p \\ h - uc_p \end{bmatrix}, \quad r_3 = \frac{1}{h + uc_p}\begin{bmatrix} 1 \\ u + c_p \\ h + uc_p \end{bmatrix}. \tag{3.62}$$

where

$$b_1 = \frac{\partial p}{\partial \rho} - \Gamma E, \quad h = E + \frac{p - s_{xx}}{\rho}. \tag{3.63}$$

Take a comparason of Eq.(3.6) and Eq.(3.61), we notice that the sonic speed is not continuous between the states of elastic and plastic. As the shear modulus $\mu$ is always positive, so the elastic wave is always faster than the plastic wave. This is very important and may cause wrong results if ignoring it.

[1] Code site link

### 3.2.2 Relations across the contact wave

According to the eigenvectors in Eq.(3.62), for the $\lambda_1$-wave ($\lambda_1 = u$), we have

$$\frac{d\rho}{\frac{-\Gamma}{b_1}} = \frac{d(\rho u)}{\frac{-u\Gamma}{b_1}} = \frac{d(\rho E)}{1}. \tag{3.64}$$

From the above equations, we can easily deduce that

$$du = 0, \quad dp = 0. \tag{3.65}$$

Samilar to that in section 3.1.3, we can also get the relations

$$s^* = u_L^* = u_R^*, \quad \sigma_L^* = \sigma_R^*. \tag{3.66}$$

### 3.2.3 Relations across rarefaction waves

***Left-going rarefaction wave*** Across the left wave associated with $\lambda_2$-wave, ($\lambda_2 = u - c_p$), we have

$$\frac{d\rho}{1} = \frac{d(\rho u)}{u - c_p} = \frac{d(\rho E)}{h - uc_p}. \tag{3.67}$$

Samilar to section 3.1.4, we can get the relations

$$pe^{\frac{\lambda}{\rho}} - \int f_2(\rho)e^{\frac{\lambda}{\rho}}d\rho = \text{constant}. \tag{3.68}$$

and

$$u + \int \frac{c_p}{\rho}d\rho = \text{constant}, \tag{3.69}$$

where

$$\lambda = \rho_0\Gamma_0 \quad f_2(\rho) = a_0^2\frac{\partial f}{\partial \eta} - \lambda\frac{s_{xx}(\rho)}{\rho^2}. \tag{3.70}$$

***Right-going rarefaction wave*** Across the right wave associated with $\lambda_3$-wave, ($\lambda_3 = u + c_e$), we have

$$\frac{d\rho}{1} = \frac{d(\rho u)}{u + c_p} = \frac{d(\rho E)}{h + uc_p}. \tag{3.71}$$

We can get similar relations as the left-going wave as

$$pe^{\frac{\lambda}{\rho}} - \int f_2(\rho)e^{\frac{\lambda}{\rho}}d\rho = \text{constant}. \tag{3.72}$$

$$u - \int \frac{c_p}{\rho}d\rho = \text{constant}. \tag{3.73}$$

### 3.2.4 Relations across shock waves

By a same deducing process with Section 3.1.5, we can get the state after a shock as

$$s_{xx2} = s_{xx1}, \tag{3.74}$$

$$p_2 = \frac{2t(c_1 f(\rho_2/\rho_0) + e_1) - (\sigma_1 + s_{xx2})}{2tc_0 - 1}, \tag{3.75}$$

where $c_0 = \frac{1}{\rho_0\Gamma_0}$ and $c_1 = \frac{a_0^2}{\Gamma_0}$.

$$\sigma_2 = -p_2 + s_{xx2}. \tag{3.76}$$

$$u_2 = \begin{cases} u_1 - \sqrt{\dfrac{\sigma_1 - \sigma_2}{t}} & \text{Left-going,} \\ u_1 + \sqrt{\dfrac{\sigma_1 - \sigma_2}{t}} & \text{Right-going.} \end{cases} \tag{3.77}$$

And the shock speed is given as

$$s = \frac{\rho_2 u_2 - \rho_1 u_1}{\rho_2 - \rho_1}. \tag{3.78}$$

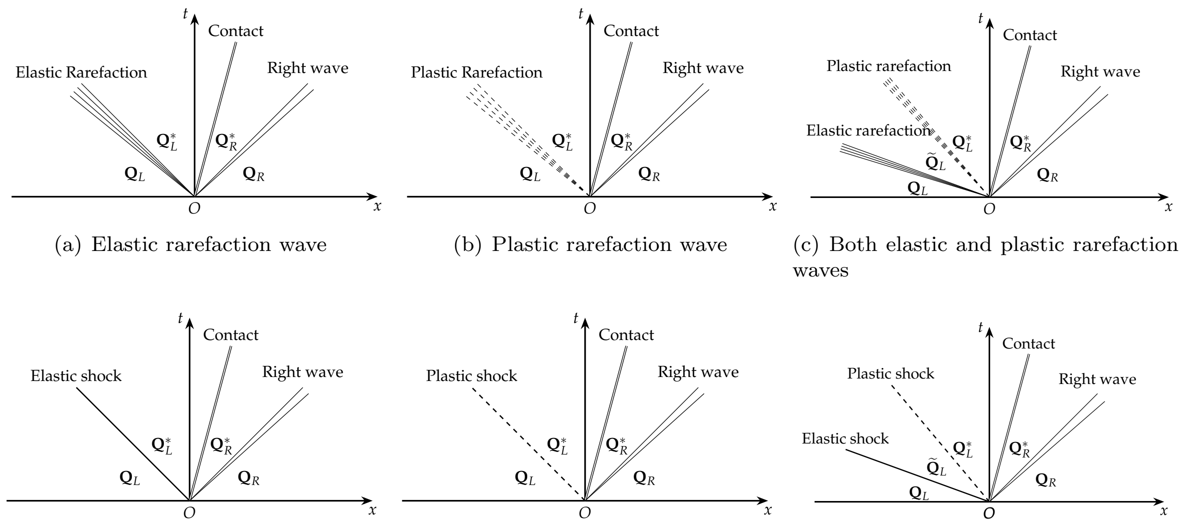


(a) Elastic rarefaction wave
(b) Plastic rarefaction wave
(c) Both elastic and plastic rarefaction waves
(d) Elastic shock wave
(e) Plastic shock wave
(f) Both elastic and plastic shock waves

Figure 1: The possible cases of Riemann solution structures in the left side.

# 4 Exact Riemann solver [2]

Now we consider the constructing details of the exact Riemann solver. For the Riemann problem in Section 4, there are $6 \times 6$ possible cases in the Riemann solution with different wave structures. The left six cases are shown in Fig.1.

## 4.1 The solving process

By those relations in Section 3, all variables can be written as functions of the density, so if densities in regions $\mathbf{Q}_L^*$ and $\mathbf{Q}_R^*$ are known, the Riemann problem is solved. e For given values of $\rho_L^*$ and $\rho_R^*$, by relations across the contact wave in Section 3.1.3 and Section 3.2.2, we can get

$$\begin{aligned} f_u(\rho_L^*, \rho_R^*) &= u_L^* - u_R^* = 0, \\ f_\sigma(\rho_L^*, \rho_R^*) &= \sigma_L^* - \sigma_R^* = 0. \end{aligned} \tag{4.1}$$

Then using a Newton iteration method, we can solve the densities $\rho_L^*$ and $\rho_R^*$ out. The solving process is shown in Fig.2, and the details are list in the following.

**Initial:**

The initial densities are given as

$$\rho_{L(0)}^* = \rho_L \quad \rho_{R(0)}^* = \rho_R. \tag{4.2}$$

**Iteration begin:**

Step 1 Case select: By a given $\rho_{L,(k)}^*$ and a $\rho_{R,(k)}^*$ in $k$ iteration step, we need to determine cases of wave structures in the left and right. The determining process is done in Section 4.2.

Step 2 Solving $f_u$ and $f_\sigma$: After determining the structure case, we need to solve the Cauchy stresses and the velocities in regions $\mathbf{Q}_L^*$ and $\mathbf{Q}_R^*$, those are given in Section 4.4.

Step 3 Updating $\rho_L^*$ and $\rho_R^*$: By the Newton iteration equation, new densities can be updated,

$$\begin{bmatrix} \rho_{L,(k+1)}^* \\ \rho_{R,(k+1)}^* \end{bmatrix} = \begin{bmatrix} \rho_{L,(k)}^* \\ \rho_{R,(k)}^* \end{bmatrix} - \begin{bmatrix} \frac{\partial f_{u(k)}}{\partial \rho_L^*} & \frac{\partial f_{u(k)}}{\partial \rho_R^*} \\ \frac{\partial f_{\sigma(k)}}{\partial \rho_L^*} & \frac{\partial f_{\sigma(k)}}{\partial \rho_R^*} \end{bmatrix}^{-1} \begin{bmatrix} f_{u(k)} \\ f_{\sigma(k)} \end{bmatrix} \tag{4.3}$$

[2] Code site link

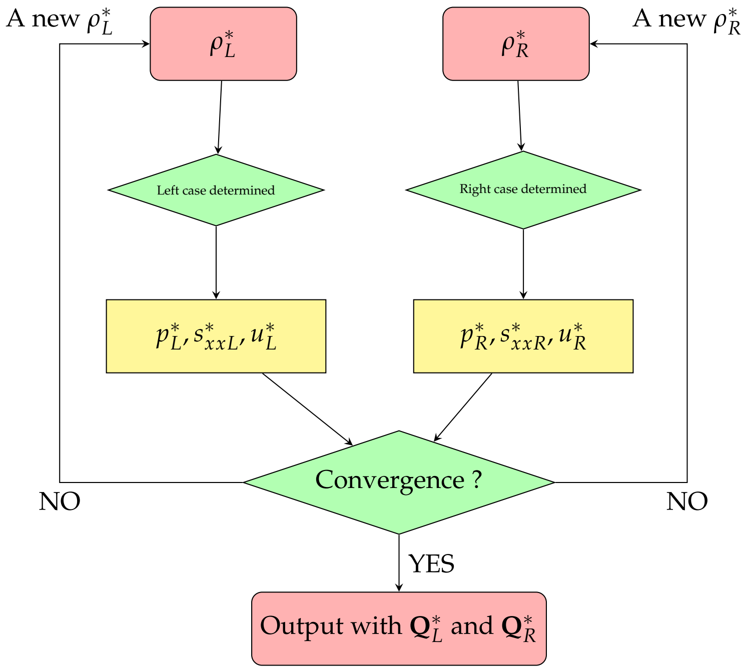


Figure 2: A flow chat of the Newton iteration process.

The derivatives of $f_u$ and $f_\sigma$ are given by

$$\frac{\partial f_{u,(k+1)}}{\partial \rho^*_{L(R)}} = \frac{f_{u,(k+1)} - f_{u,(k)}}{\rho^*_{L(R),(k+1)} - \rho_{L(R),(k)}}, \quad \frac{\partial f_{\sigma,(k+1)}}{\partial \rho^*_{L(R)}} = \frac{f_{\sigma,(k+1)} - f_{\sigma,(k)}}{\rho^*_{L(R),(k+1)} - \rho_{L(R),(k)}}, \tag{4.4}$$

At the first step, we use a simple numerical difference method

$$\frac{\partial f_{u,(1)}}{\partial \rho^*_{L(R)}} = \frac{f_u(\rho^*_{L(R)} + \Delta\rho) - f_u(\rho^*_{L(R)})}{\Delta \rho_{L(R)}}, \quad \frac{\partial f_{u,(1)}}{\partial \rho^*_{L(R)}} = \frac{f_u(\rho^*_{L(R)} + \Delta\rho) - f_u(\rho^*_{L(R)})}{\Delta \rho_{L(R)}}, \tag{4.5}$$

where $\Delta\rho$ is a little quatity, we can choose it as

$$\Delta\rho_{L(R)} = \frac{\rho^*_{L(R),(0)}}{100}. \tag{4.6}$$

Step 4 Convergence test: The convergence is meassured by

$$\text{CHA} = \max\left[\frac{|\rho^*_{L(k+1)} - \rho^*_{L,(k)}|}{\frac{1}{2}|\rho^*_{L(k+1)} + \rho^*_{L(k)}|}, \frac{|\rho^*_{R(k+1)} - \rho^*_{R,(k)}|}{\frac{1}{2}|\rho^*_{R(k+1)} + \rho^*_{R(k)}|}, |f_u|, |f_\sigma|\right]. \tag{4.7}$$

and the tolerance is taken as $\text{TOL} = 10^{-4}$.

If $\text{CHA} \leq \text{TOL}$, the iteration ends. It usually takes 2-4 steps to get a convergence result.

**Iteration end**

## 4.2 Determining the case of structures

Using a given density $\rho^*_{L(R)}$ we can distinguish the shock and rarefaction wave. This is done easily by comparing $\rho^*_{L(R)}$ with $\rho_{L(R)}$, the subscript $_{L(R)}$ means either both in the left side $_L$ and right side $_R$.

$$\begin{cases} \text{Rarefaction wave:} & \rho_{L(R)} > \rho^*_{L(R)}, \\ \text{Shock wave:} & \rho_{L(R)} < \rho^*_{L(R)}. \end{cases} \tag{4.8}$$

Table 4.1: The condition of cases classification.

| Conditions | $\|s_{xx}\| < \frac{2}{3}Y_0$ and $\|\hat{s}_{xx}\| < \frac{2}{3}Y_0$ | $s_{xx} = \frac{2}{3}Y_0$ | other |
|---|---|---|---|
| $\hat{\rho^*} < \rho$ | case a | case b | case c |
| $\hat{\rho^*} > \rho$ | case d | case e | case f |

To determine the number of waves, we need to know the yielding situation, the devaitoric stress can be evaluated as

$$\hat{s}_{xxL(R)} = -\frac{4}{3}\mu \ln\left(\frac{\rho^*_{L(R)}}{\rho_{L(R)}}\right) + s_{xxL(R)}, \tag{4.9}$$

Then we can classify every side into six cases, and conditions for the classfication are shown in Table 4.1, the subscripts $_L$ and $_R$ are omitted for simplication.

## 4.3 States in regions $\tilde{\mathbf{Q}}_L$ and $\tilde{\mathbf{Q}}_R$

For cases (a,b,d,e) in Fig.1, the material is totally yielding or totally not yielding, there is no midlle state $\tilde{\mathbf{Q}}_{L(R)}$. For expression conveience, we let

$$(\tilde{\rho}_{L(R)}, \tilde{u}_{L(R)}, \tilde{p}_{L(R)}, \tilde{s}_{xx}) = (\rho_{L(R)}, u_{L(R)}, p_{L(R)}, s_{xxL(R)}), \tag{4.10}$$

For cases (c,f), the meterial periods a yielding process from elastic to plastic. There are two waves and one more state $\tilde{\mathbf{Q}}_{L(R)}$ exist. In state $\tilde{\mathbf{Q}}_{L(R)}$, the derivative stress achieves the elastic limit.

$$\tilde{s}_{xxL(R)} = \begin{cases} \frac{2}{3}Y_0 & \text{Case (c),} \\ -\frac{2}{3}Y_0 & \text{Case (f),} \end{cases} \tag{4.11}$$

By the relation in (3.13), we can solve the density out as

$$\tilde{\rho}_{L(R)} = \begin{cases} \rho_{L(R)} \exp\left(-\frac{Y_0}{2\mu} + \frac{3s_{xxL(R)}}{4\mu}\right), & \text{Case (c),} \\ \rho_{L(R)} \exp\left(\frac{Y_0}{2\mu} + \frac{3s_{xxL(R)}}{4\mu}\right), & \text{Case (f).} \end{cases} \tag{4.12}$$

***Rarefaction wave case (c)*** For rarefaction wave case, we give the function of $s_{xx}$ at first,

$$s_{xx}(\rho) = -\frac{4}{3}\mu \ln\left(\frac{\rho}{\rho_{L(R)}}\right) + s_{xxL(R)} \quad \rho_{L(R)} \geq \rho \geq \tilde{\rho}_{L(R)} \tag{4.13}$$

The pressure is given as

$$p(\rho) = p_{L(R)} e^{\frac{\lambda}{\rho_{L(R)}} - \frac{\lambda}{\rho}} + e^{-\frac{\lambda}{\rho}} \int_{\rho_{L(R)}}^{\rho} f_2(x) e^{\frac{\lambda}{x}} dx, \quad \rho_{L(R)} \geq \rho \geq \tilde{\rho}_{L(R)}, \tag{4.14}$$

where

$$\lambda = \rho_0 \Gamma_0 \quad f_2(\rho) = a_0^2 \frac{\partial f}{\partial \eta} - \lambda \frac{s_{xx}(\rho)}{\rho^2}. \tag{4.15}$$

And sonic speed,

$$c_e(\rho) = \sqrt{a_0^2 \frac{\partial f}{\partial \eta} + \frac{p(\rho)}{\rho^2}\rho_0\Gamma_0 - \frac{\rho_0}{\rho^2}\Gamma_0 s_{xx}(\rho) + \frac{4}{3}\frac{\mu}{\rho}} \quad \rho_{L(R)} \geq \rho \geq \tilde{\rho}_{L(R)} \tag{4.16}$$

Then we can get the function of velocity

$$u(\rho) = \begin{cases} u_L - \displaystyle\int_{\rho_L}^{\rho} \frac{c(x)}{x} dx, & \rho_L \geq \rho \geq \tilde{\rho}_L, \\ u_R + \displaystyle\int_{\rho_R}^{\rho} \frac{c(x)}{x} dx, & \rho_R \geq \rho \geq \tilde{\rho}_R, \end{cases} \quad \text{case (c).} \tag{4.17}$$

States in region $\tilde{\mathbf{Q}}_{L(R)}$ can be solved as

$$\tilde{s}_{xxL(R)} = s_{xx}(\rho_{L(R)}), \quad \tilde{p}_{L(R)} = p(\rho_{L(R)}), \quad \tilde{u}_{L(R)} = u(\rho_{L(R)}). \tag{4.18}$$

***Shock wave case (f)*** For shock wave case, the deviatoric stress is given as

$$\tilde{s}_{xxL(R)} = -\frac{4}{3}\mu \ln\left(\frac{\tilde{\rho}_{L(R)}}{\rho_{L(R)}}\right) + s_{xxL(R)} \tag{4.19}$$

Then the pressure can be solved as

$$\tilde{p}_{L(R)} = \frac{2t(c_1 f(\tilde{\rho}_{L(R)}/\rho_0) + e_L) - (\sigma_{L(R)} + \tilde{s}_{xxL(R)})}{2tc_0 - 1}, \tag{4.20}$$

where $c_0 = \frac{1}{\rho_0 \Gamma_0}$, $c_1 = \frac{a_0^2}{\Gamma_0}$ and $t = \frac{\rho_{L(R)}\tilde{\rho}_{L(R)}}{\tilde{\rho}_{L(R)} - \rho_{L(R)}}$.

At last the velocity is

$$\begin{cases} \tilde{u}_L = u_L - \sqrt{\frac{\sigma_L - \tilde{\sigma}_L}{t}}, \\ \tilde{u}_R = u_R + \sqrt{\frac{\sigma_R - \tilde{\sigma}_R}{t}}, \end{cases} \tag{4.21}$$

where

$$\tilde{\sigma}_{L(R)} = -\tilde{p}_{L(R)} + \tilde{s}_{L(R)}. \tag{4.22}$$

## 4.4 States in regions $\mathbf{Q}_L^*$ and $\mathbf{Q}_R^*$

***Rarefaction wave*** For rarefaction wave, we not only need to solve the state after the wave in region $\mathbf{Q}_{L(R)}^*$, but also need to know states inside the expansion region.

First we give the function of $s_{xx}$,

$$s_{xx}(\rho) = \begin{cases} -\dfrac{4}{3}\mu \ln\left(\dfrac{\rho}{\tilde{\rho}_{L(R)}}\right) + s_{xxL(R)}, & \tilde{\rho}_{L(R)} \geq \rho \geq \rho_{L(R)}^*, \quad \text{case (a),} \\ \dfrac{2}{3}Y_0, & \tilde{\rho}_{L(R)} \geq \rho \geq \rho_{L(R)}^*, \quad \text{case (b,c).} \end{cases} \tag{4.23}$$

Then we give the pressure,

$$p(\rho) = \tilde{p}_{L(R)} e^{\frac{\lambda}{\tilde{\rho}_{L(R)}} - \frac{\lambda}{\rho}} + e^{-\frac{\lambda}{\rho}} \int_{\tilde{\rho}_{L(R)}}^{\rho} f_2(x) e^{\frac{\lambda}{x}} dx, \quad \tilde{\rho}_{L(R)} \geq \rho \geq \rho_{L(R)}^* \tag{4.24}$$

where

$$\lambda = \rho_0 \Gamma_0 \quad f_2(\rho) = a_0^2 \frac{\partial f}{\partial \eta} - \lambda \frac{s_{xx}(\rho)}{\rho^2}. \tag{4.25}$$

And sonic speed,

$$c(\rho) = \begin{cases} \sqrt{a_0^2 \dfrac{\partial f}{\partial \eta} + \dfrac{p(\rho)}{\rho^2}\rho_0\Gamma_0 - \dfrac{\rho_0}{\rho^2}\Gamma_0 s_{xx}(\rho) + \dfrac{4}{3}\dfrac{\mu}{\rho}} & \text{case (a),} \\ \sqrt{a_0^2 \dfrac{\partial f}{\partial \eta} + \dfrac{p(\rho)}{\rho^2}\rho_0\Gamma_0 - \dfrac{\rho_0}{\rho^2}\Gamma_0 s_{xx}(\rho)} & \text{case (b,c).} \end{cases} \tag{4.26}$$

Then we can get the function of velocity

$$u(\rho) = \begin{cases} \tilde{u}_L - \displaystyle\int_{\rho_L}^{\rho} \frac{c(x)}{x} dx, & \tilde{\rho}_L \geq \rho \geq \rho_L^*, \\ \tilde{u}_R + \displaystyle\int_{\rho_R}^{\rho} \frac{c(x)}{x} dx, & \tilde{\rho}_R \geq \rho \geq \rho_R^*, \end{cases} \tag{4.27}$$

By now, we can get the state in star regions as

$$p_{L(R)}^* = p(\rho_{L(R)}^*), \quad s_{xxL(R)}^* = s_{xx}(\rho_{L(R)}^*), \quad u_{L(R)}^* = u(\rho_{L(R)}^*). \tag{4.28}$$

***Shock wave*** For shock waves, the deviatoric stress is given as

$$s_{xx}(\rho) = \begin{cases} -\dfrac{4}{3}\mu \ln\left(\dfrac{\rho}{\tilde{\rho}_{L(R)}}\right) + \tilde{s}_{xxL(R)}, & \text{case (d)}, \\ -\dfrac{2}{3}Y_0, & \text{cases (e, f)}. \end{cases} \tag{4.29}$$

And the pressure is given as

$$p(\rho) = \frac{2t(c_1 f(\rho/\rho_0) + \tilde{e}_{L(R)}) - (\tilde{\sigma}_{L(R)} + s_{xx}(\rho))}{2tc_0 - 1}, \tag{4.30}$$

where $c_0 = \frac{1}{\rho_0 \Gamma_0}$ and $c_1 = \frac{a_0^2}{\Gamma_0}$ and $t = \frac{\tilde{\rho}_{L(R)}\rho}{\rho - \tilde{\rho}_{L(R)}}$. And the velocity is given as

$$u(\rho) = \begin{cases} \tilde{u}_L - \sqrt{\frac{\tilde{\sigma}_L - \sigma(\rho)}{t}}, \\ \tilde{u}_R + \sqrt{\frac{\tilde{\sigma}_R - \sigma(\rho)}{t}}, \end{cases} \tag{4.31}$$

where $\sigma(\rho) = -p(\rho) + s_{xx}(\rho)$. And the state in the star region is given as

$$p_{L(R)}^* = p(\rho_{L(R)}^*), \quad s_{xxL(R)}^* = s_{xx}(\rho_{L(R)}^*), \quad u_{L(R)}^* = u(\rho_{L(R)}^*). \tag{4.32}$$

# 5 Half Riemann problem and its solver

Some time we need to analyse a half Riemann problem with a given velocity or Cauchy stress. Shown in Fig.3 , in these cases, we only need to solve states in one side. There are six possible cases just like them in Section 4.

As we know the velocity $u^*$ or the Cauchy stress $\sigma^*$, there is only one function need to be solved as

$$f(\rho^*) = u(\rho^*) - u^* = 0, \tag{5.1}$$

or

$$f(\rho^*) = \sigma(\rho^*) - \sigma^* = 0. \tag{5.2}$$

The solving process is list in the following.

**Initial:**

The initial density is given as

$$\rho_{(0)}^* = \rho_R. \tag{5.3}$$

**Iteration begin:**

Step 1 Case select: By a given $\rho_{(k)}^*$ in $k$ iteration step, we need to determine the case of the wave structures in the left side. The determining process is also done in Section 4.2.

Step 2 Solving $f$: After determining the structure case, we need to solve the velocity ( or the Cauchy stress) in the region $\mathbf{Q}^*$, this is given in Section 4.4.

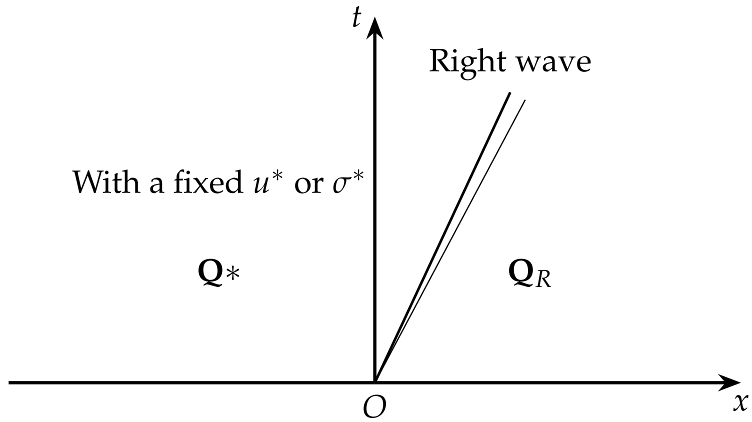


Figure 3: Half Riemann problem with a given left velocity or Cauchy stress..

Step 3 Updating $\rho^*$: By the Newton iteration equation, a new density can be updated as

$$\rho^*_{(k+1)} = \rho^*_{(k)} - f / \frac{\partial f_{(k)}}{\partial \rho}, \tag{5.4}$$

The derivatives of $f$ is given by

$$\frac{\partial f_{(k+1)}}{\partial \rho^*} = \frac{f_{(k+1)} - f_{(k)}}{\rho^*_{(k+1)} - \rho^*_{(k)}}, \tag{5.5}$$

At the first step, we use a simple numerical difference method

$$\frac{\partial f_{(1)}}{\partial \rho^*} = \frac{f(\rho^* + \Delta\rho) - f(\rho^*)}{\Delta\rho}, \tag{5.6}$$

where $\Delta\rho$ is a little quatity, we can choose it as

$$\Delta\rho = \frac{\rho^*_{(0)}}{100}. \tag{5.7}$$

Step 4 Convergence test: The convergence is meassured by

$$\mathrm{CHA} = \max\left[\frac{|\rho^*_{(k+1)} - \rho^*_{(k)}|}{\frac{1}{2}|\rho^*_{(k+1)} + \rho^*_{(k)}|}, |f|\right]. \tag{5.8}$$

and the tolerance is taken as $\mathrm{TOL} = 10^{-4}$.

If $\mathrm{CHA} \le \mathrm{TOL}$, the iteration ends. It usually takes 2-4 step to get a convergence result.

**Iteration end.**

# 6 Numerical tests

In this section, by choosing suitable initial conditions, we will solve the Riemann problem with several different structure cases in the solution. For simple expression, in figures, we use same representations as those in [9]. "|" means the contact wave, and capital letters "S" and "R" means the shock and rarefaction wave. Superscript letters "E" and "P" indicate the elastic or plastic state of a wave. Numerical results by the method in [5] is used to verified the correctness of the exact solution. In the following tests, the materials are taken as aluminium and copper. The parameters for the EOS and constitutive model for aluminum and copper are $(\rho_0, a_0, \Gamma_0, s, \mu)_{\mathrm{Al}} = (8930\mathrm{kg/m}^3, 3940\mathrm{m/s}, 2, 1.49, 2.76, 2.76\times10^{10}\mathrm{Pa})$ and $(\rho_0, a_0, \Gamma_0, s, \mu)_{\mathrm{copper}} = (2785\mathrm{kg/m}^3, 5328\mathrm{m/s}, 2, 1.338, 4.5\times10^{10}\mathrm{Pa})$, respectively. The computational domain is set to be $[0, 1m]$ with 800 cell points and the intial interface is located at $0.5m$, the terminal time is $t = 5\times10^{-5}s$.

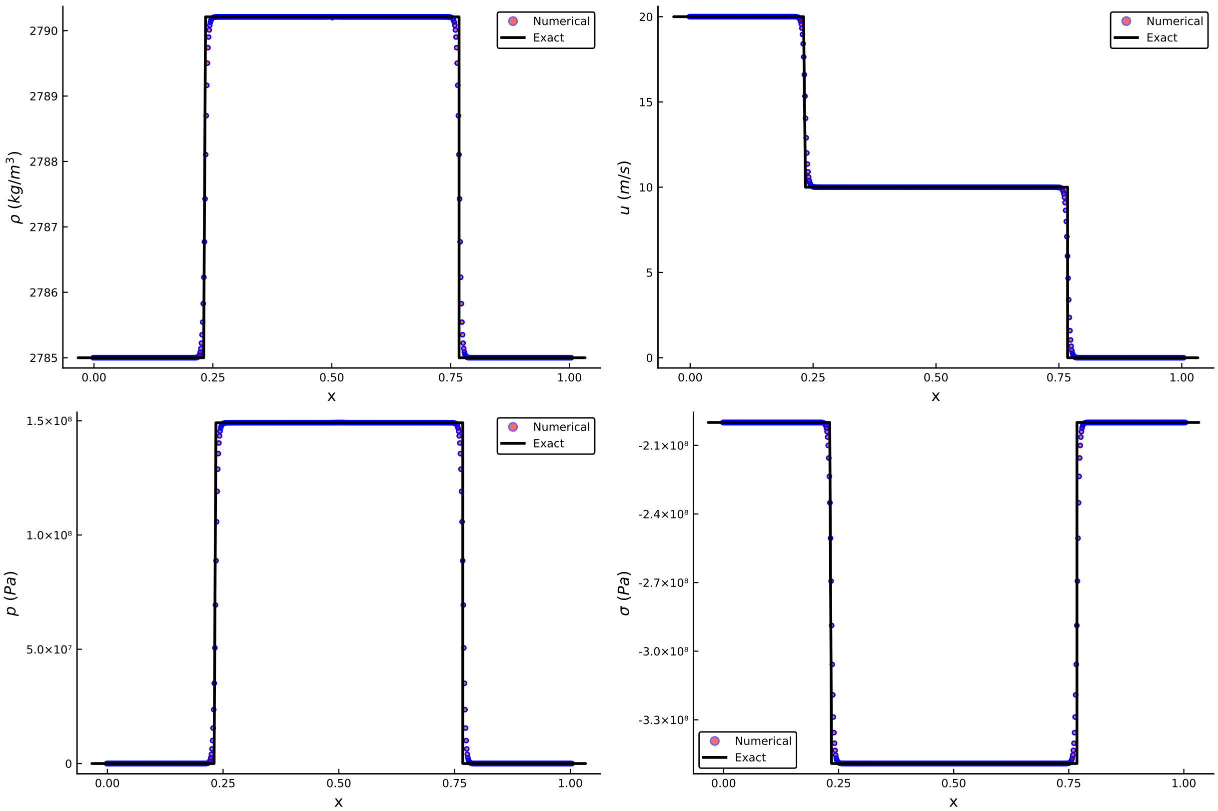


Figure 4: Comparison resutls for Test 1 with the structrures of $S^P|S^P$.

## 6.1 Test 1

In this case, the material is yielding at both sides, so the solution structure has three wave with two plastic waves and one contact. The initial condition is

$$\begin{cases} \text{L: Al}, \quad \rho = 2785\text{kg/m}^3, \quad u = 20\text{m/s}, \quad p = 1.0\text{Pa}, \quad s_{xx} = -2.0 \times 10^8\text{Pa}, \\ \text{R: Al}, \quad \rho = 2785\text{kg/m}^3, \quad u = 0\text{m/s}, \quad p = 1.0\text{Pa}, \quad s_{xx} = -2.0 \times 10^8\text{Pa}, \end{cases} \tag{6.1}$$

It can be seen that the exact solution matches the numerical results very well in Fig.4.

## 6.2 Test 2

Next, we consider a case with yielding process at both sides, so the result has five waves. The initial condition is

$$\begin{cases} \text{L: Al}, \quad \rho = 2785\text{kg/m}^3, \quad u = 800\text{m/s}, \quad p = 1.0\text{Pa}, \quad s_{xx} = 0.0\text{Pa}, \\ \text{R: Al}, \quad \rho = 2785\text{kg/m}^3, \quad u = 0\text{m/s}, \quad p = 1.0\text{Pa}, \quad s_{xx} = 0.0\text{Pa}, \end{cases} \tag{6.2}$$

Shown in Fig.5, the exact solution matches the numerical results well generally, besides the under-cooling effect performed in the numerical results, but it is not considered in the designing of the exact Riemann solver.

## 6.3 Test 3

In this example, we test the elastic rarefaction waves case. In the structrues there is one elastic rarefaction wave on each side of the contace wave. The initial condition is given as

$$\begin{cases} \text{L: Al}, \quad \rho = 2785\text{kg/m}^3, \quad u = -2.0\text{m/s}, \quad p = 1.0^7\text{Pa}, \quad s_{xx} = 0.0\text{Pa}, \\ \text{R: Al}, \quad \rho = 2785\text{kg/m}^3, \quad u = 2.0\text{m/s}, \quad p = 1.0 \times 10^7\text{Pa}, \quad s_{xx} = 0.0\text{Pa}, \end{cases} \tag{6.3}$$

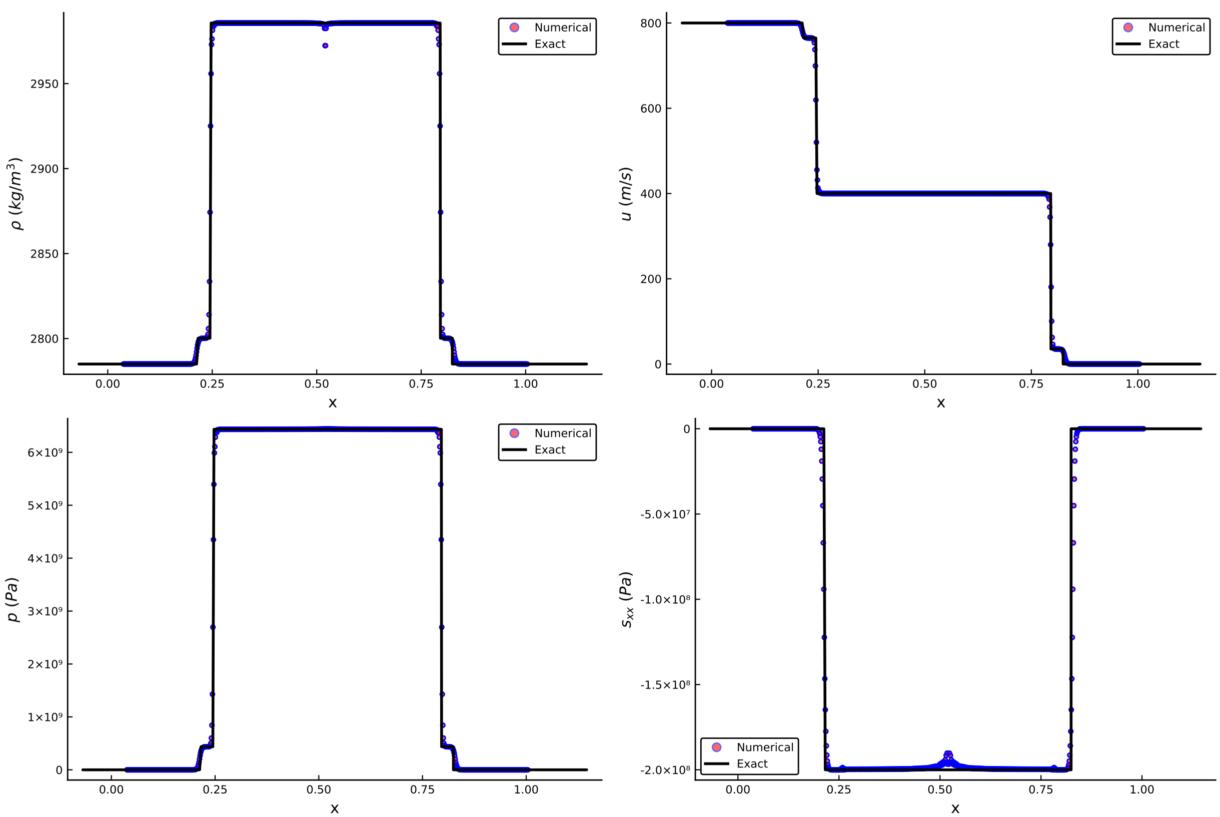


Figure 5: Comparison resutls for Test 1 with the structrures of $S^E S^P | S^P S^E$.

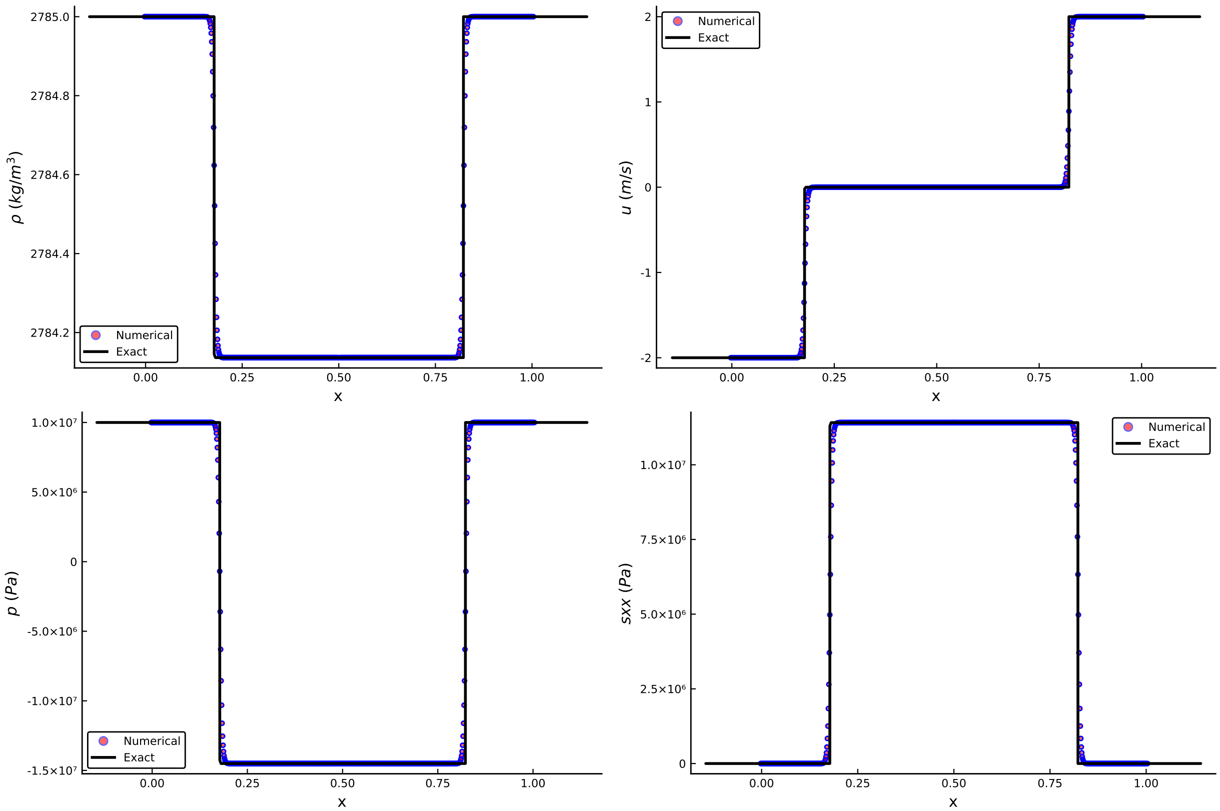


Figure 6: Comparison resutls for Test 3 with the structrures of $R^E|R^E$.

We can see that the results of the exact solution match the numerical results very well.

## 6.4 Test 4

Then we test another example with both elastic and plastic rarefaction waves on both sides. The initial condition is

$$\begin{cases} \text{L: Al}, \quad \rho = 2785\text{kg/m}^3, \quad u = -40\text{m/s}, \quad p = 1.0 \times 10^7\text{Pa}, \quad s_{xx} = 0.0\text{Pa}, \\ \text{R: Al}, \quad \rho = 2785\text{kg/m}^3, \quad u = 40\text{m/s}, \quad p = 1.0 \times 10^7\text{Pa}, \quad s_{xx} = 0.0\text{Pa}. \end{cases} \tag{6.4}$$

Results are shown in Fig.7, the results of the exact solver matches the numerical results very well.

## 6.5 Test 5

All the above four tests have symmetrical wave structrues, next we will test an example with different structrues on different sides. The initial condition is given as

$$\begin{cases} \text{L: Al}, \quad \rho = 2785\text{kg/m}^3, \quad u = 40\text{m/s}, \quad p = 1.0 \times 10^8\text{Pa}, \quad s_{xx} = -2.0 \times 10^8\text{Pa}, \\ \text{R: Al}, \quad \rho = 2785\text{kg/m}^3, \quad u = -40\text{m/s}, \quad p = 1.0 \times 10^2\text{Pa}, \quad s_{xx} = 0.0\text{Pa}. \end{cases} \tag{6.5}$$

In the Fig.8 shown in both the numerical and exact solutions, there is one plastic shock on the left side and both the elastic and plastic shocks exist on the right.

## 6.6 Test 6

In this test, we consider an example with zero initial velocities on both sides, driving by the gradient of the pressure, there are rarefaction waves producted into the higher pressure side and shock waves generated into

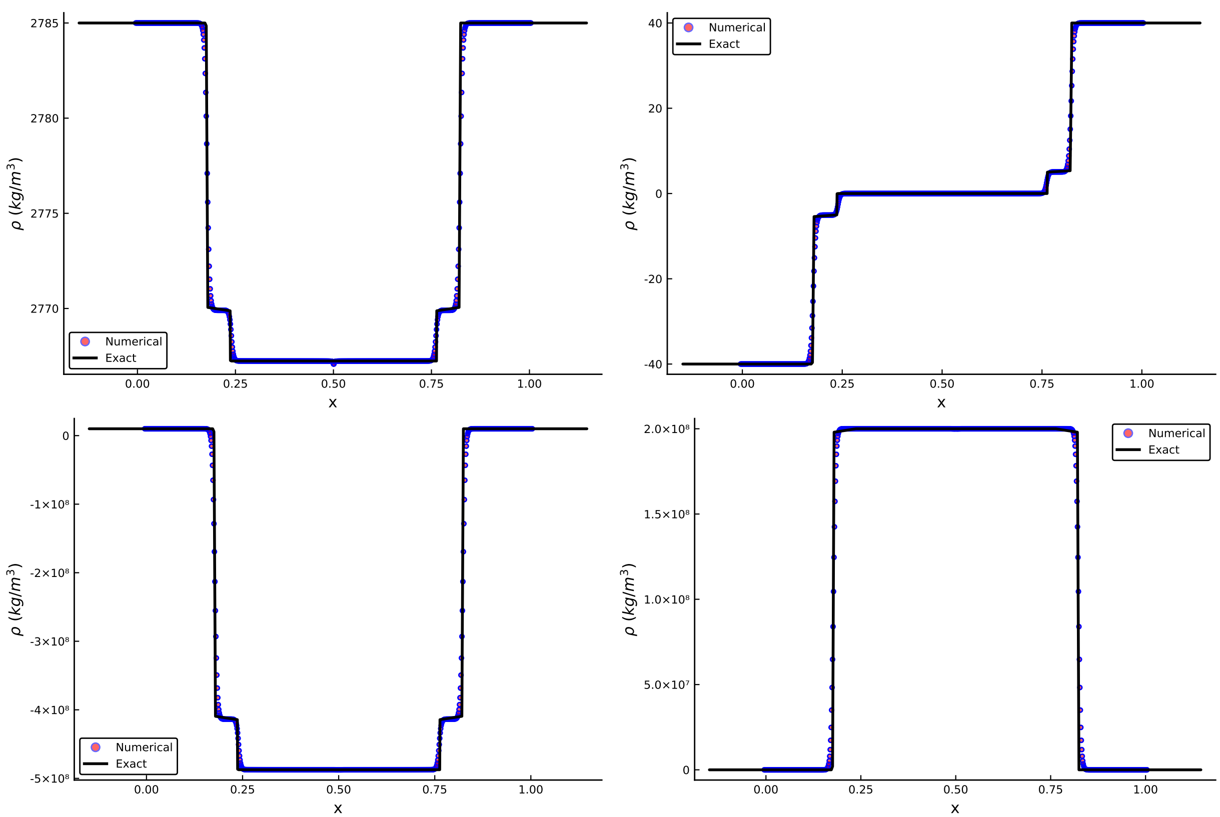


Figure 7: Comparison resutls for Test 4 with the structrures of $R^E R^P | R^P R^E$.

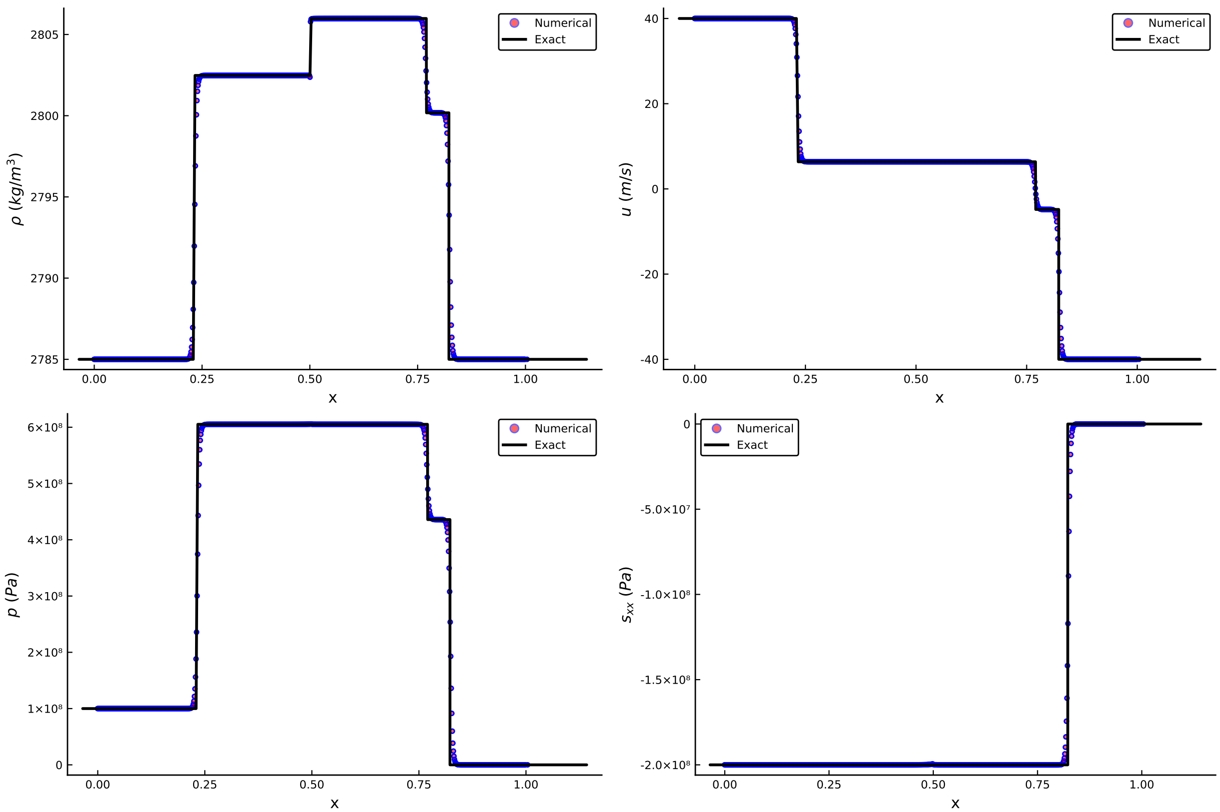


Figure 8: Comparison resutls for Test 5 with the structrures of $R^P|R^P R^E$.

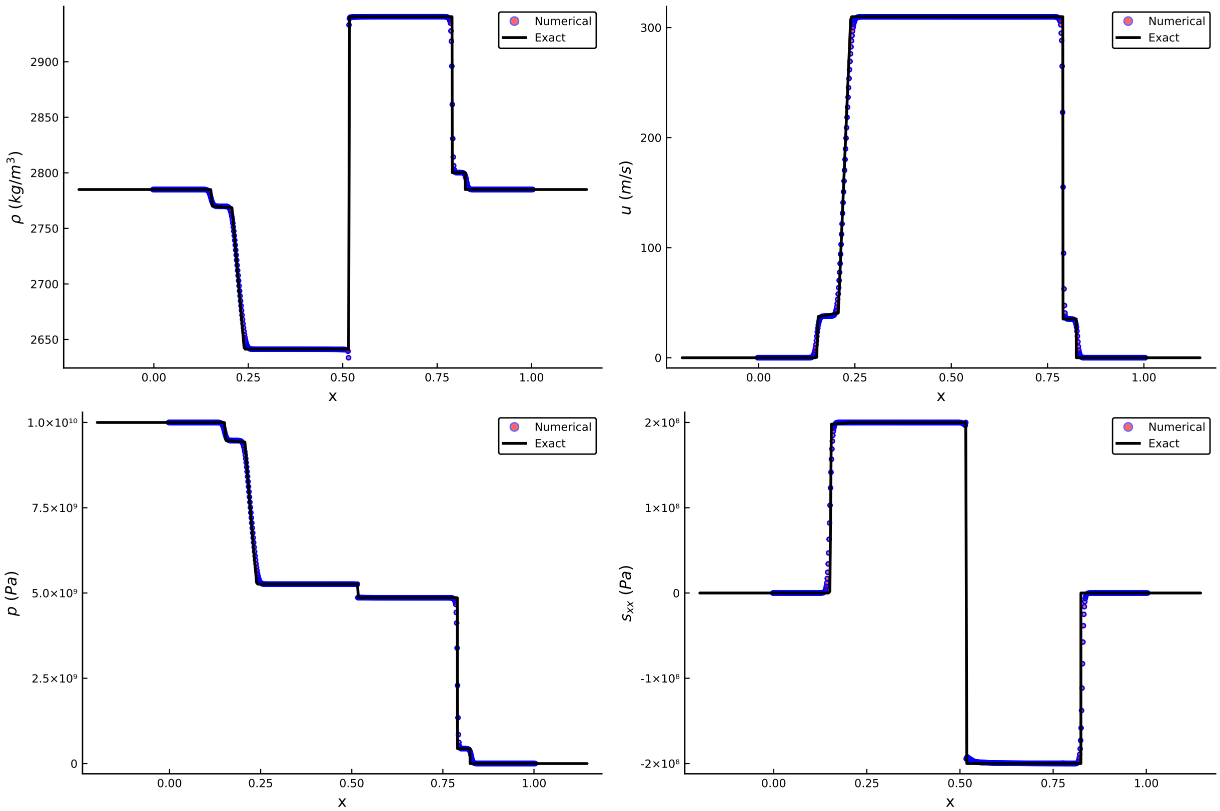


Figure 9: Comparison resutls for Test 6 with the structrures of $R^E R^P | S^P S^E$.

the lower pressure side. The initial condition is given as

$$\begin{cases} \text{L: Al}, \quad \rho = 2785\text{kg/m}^3, \quad u = 0.0\text{m/s}, \quad p = 1.0 \times 10^{10}\text{Pa}, \quad s_{xx} = 0.0\text{Pa}, \\ \text{R: Al}, \quad \rho = 2785\text{kg/m}^3, \quad u = 0.0\text{m/s}, \quad p = 1.0 \times 10^{2}\text{Pa}, \quad s_{xx} = 0.0\text{Pa}. \end{cases} \tag{6.6}$$

Shown in Fig.12, we can see there are two shocks in the right side and two rarefaction waves on the left side.

## 6.7 Test 7

Now we will consider two multi-material tests with different materials on different sides. In this test, on the left side, a lighter material of aluminum with a velocity impacts to a heavier material of copper. The initial condition is given as

$$\begin{cases} \text{L: Al}, \quad \rho = 2785\text{kg/m}^3, \quad u = 40\text{m/s}, \quad p = 0.1\text{Pa}, \quad s_{xx} = 0.0\text{Pa}, \\ \text{R: Copper}, \quad \rho = 8930\text{kg/m}^3, \quad u = 0.0\text{m/s}, \quad p = 0.1\text{Pa}, \quad s_{xx} = 0.0\text{Pa}. \end{cases} \tag{6.7}$$

Show in the Fig.10, there is a large jump of density at the material interface and both elastic shock and plastic shock exist in each side of the interface. The exact Riemann solver can solve the Riemann problem with multi-materials very well comparing to the MHLLCEP approximate solver.

## 6.8 Test 8

At last, we test another multi-materials case, in this test the initial condtion is given as

$$\begin{cases} \text{L: Copper}, \quad \rho = 8930\text{kg/m}^3, \quad u = 0.0\text{m/s}, \quad p = 1.0 \times 10^{10}\text{Pa}, \quad s_{xx} = 0.0\text{Pa}, \\ \text{R: Al}, \quad \rho = 2785\text{kg/m}^3, \quad u = 0\text{m/s}, \quad p = 10.0\text{Pa}, \quad s_{xx} = 0.0\text{Pa}. \end{cases} \tag{6.8}$$

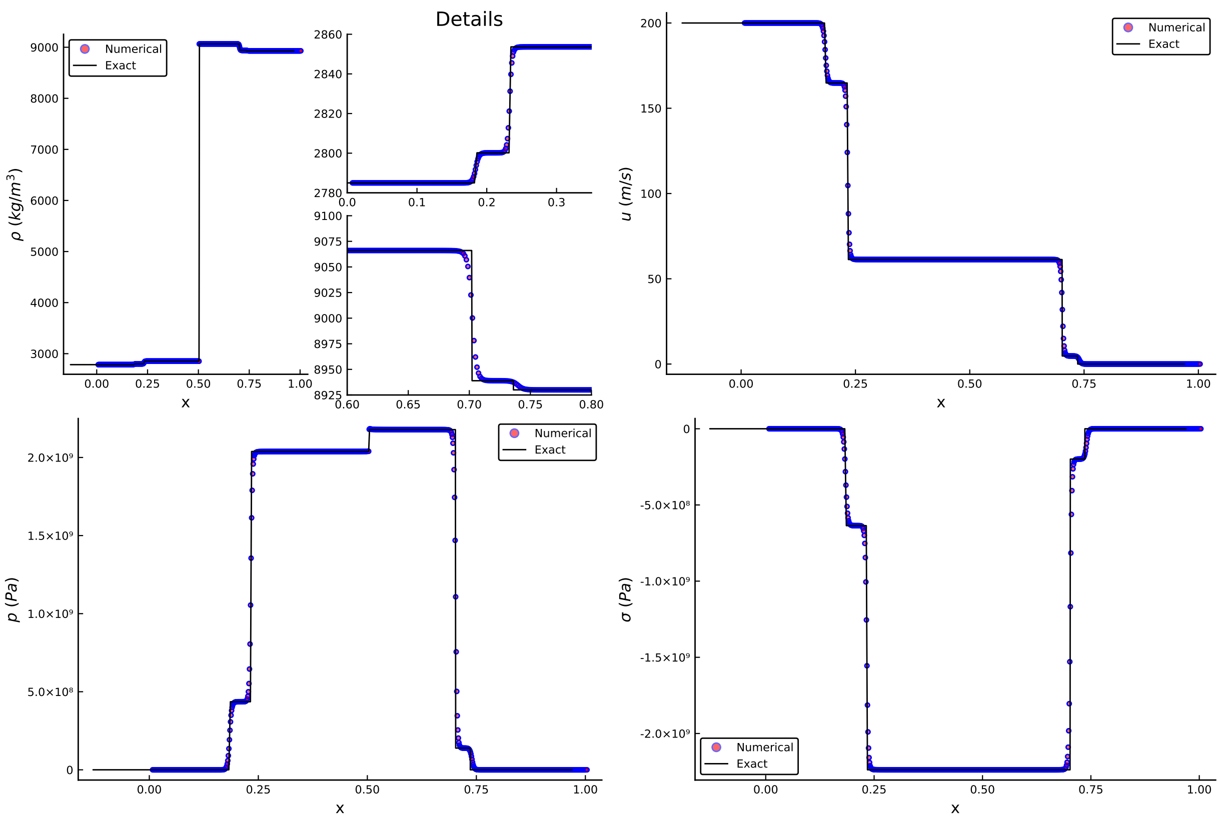


Figure 10: Comparison results for Test 7 with structrures of $R^E R^P | R^P R^E$.

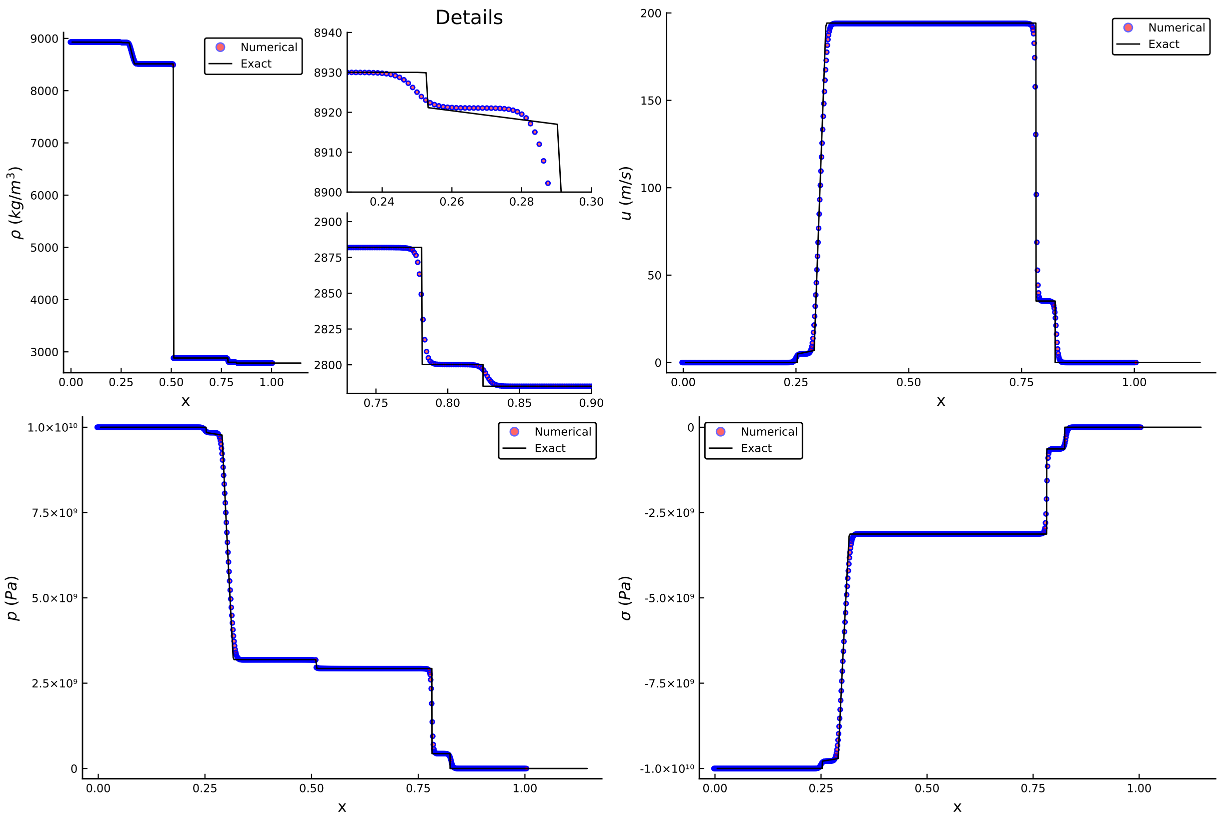


Figure 11: Comparison results for Test 8 with the structrures of $R^E R^P|S^E S^P$.

Shown in Fig.11, there are two rarefaction waves on the left side and two shocks on the right side, there is a discontinuity of pressure on the interface, and the Cauchy stress is continuous, which meets with the theoretical analysis.

### 6.9 Test 9

Then we give two tests of half Riemann problem, the first is with a given left velocity $u^* = -20\text{m/s}$, and the right initial condition is

$$\text{Copper}, \quad \rho = 8930\text{kg/m}^3, \quad u = 0.0\text{m/s}, \quad p = 0.1\text{Pa}, \quad s_{xx} = 0.0\text{Pa}. \tag{6.9}$$

In Fig.12, comparason results are given by the exact half Riemann solver and the numerical method. We can see that the exact solver can resolve both the elastic and plastic shock waves well.

### 6.10 Test 10

The second half Riemann case is with a given left Cauchy stress $\sigma^* = 0\text{Pa}$, and the right initial condition is

$$\text{Copper}, \quad \rho = 8930\text{kg/m}^3, \quad u = 0.0\text{m/s}, \quad p = 1.0\times10^9\text{Pa}, \quad s_{xx} = 0.0\text{Pa}. \tag{6.10}$$

In Fig.13, we give the results computed by the exact Riemann solver and the numerical simulation, shown in it, the exact solver can resolve the elastic and plastic rarefaction waves well.

## 7 Results

In this paper, we give a detailed analysis of the Riemann problem for one-dimensional multi-material elastic-plastic flows with the Mie-Grüneisen EOS, hypo-elastic constitutive model and the von Mises' yielding con-

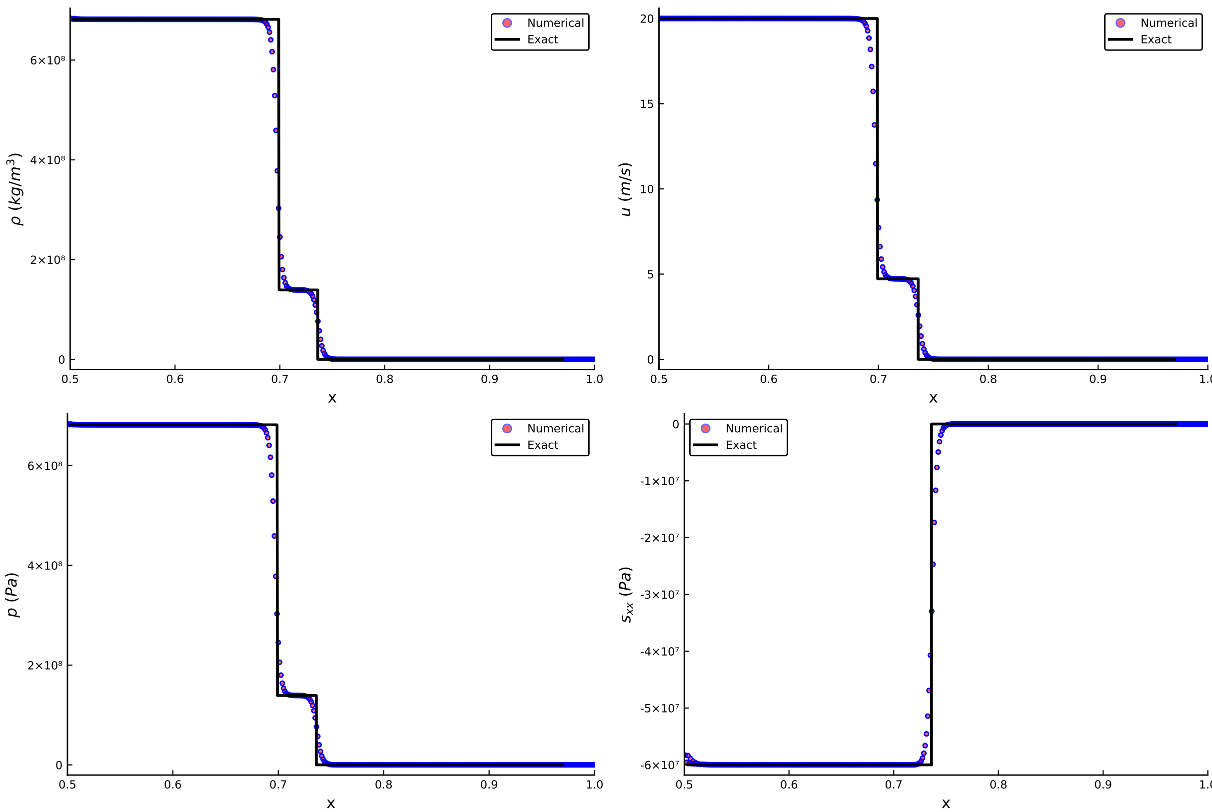


Figure 12: Comparison results for Test 9 with the structrures of $S^E S^P$.

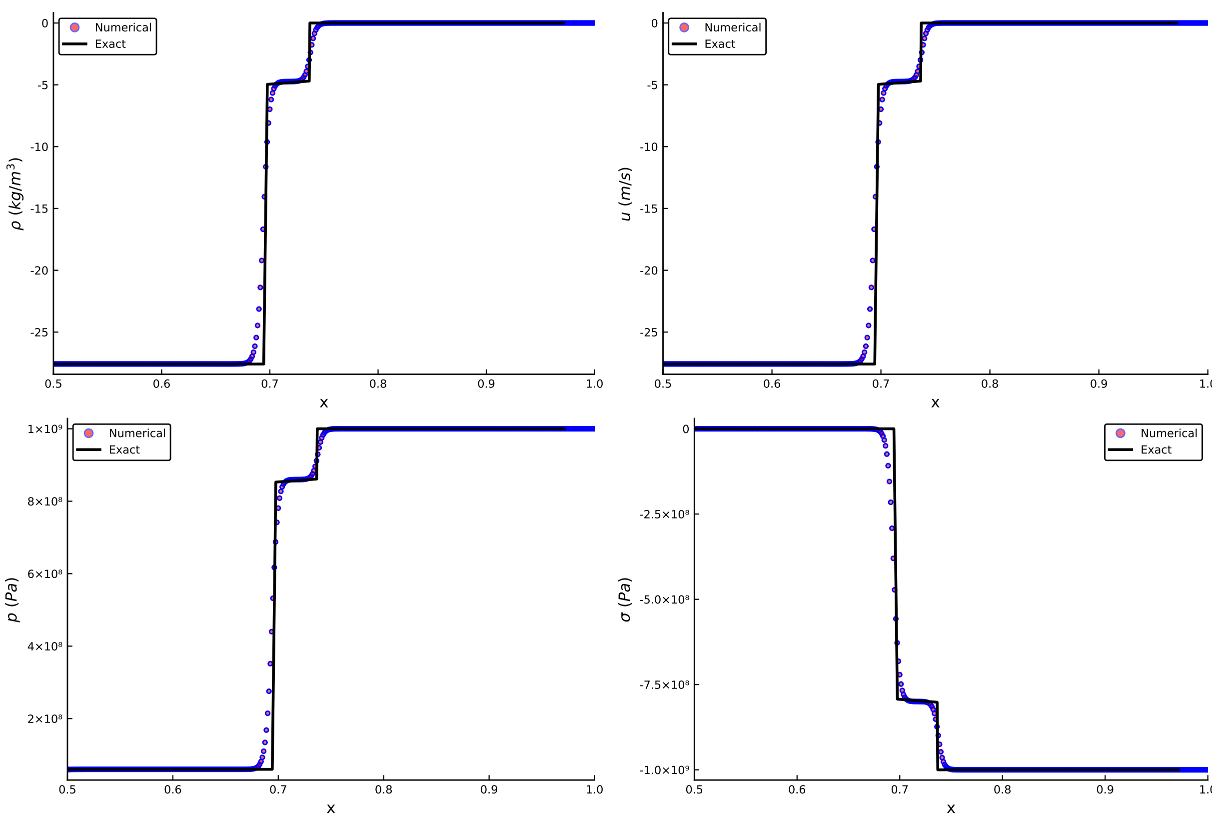


Figure 13: Comparison results for Test 10 with the structrures of $R^E R^P$.

dition. Some useful results are found through the analysing:

1. The sonic speed periods a significant jump when the material is yielding.
2. the plastic wave is always faster than the elastic wave for the reason of the sonic speed jump.
3. There are only thirty-six possible cases of the structrues in the Riemann problem.
4. All the variables after the wave can be written as functions of the density theoretically.

Then, based on the analysis, we have constructed exact Riemann solvers for both the Riemann problem and the half Riemann problem, separately, by an Newton iteration process. Tested by a large number of examples, the exact Riemann solver is reasonable and matching well with the numerical method for both the single material problem and multi-material Riemann problems.

# Acknowledgement

This work was supported by NSFC(Grant No. 11672047) and Science Challenge Project (Grant No. TZ2016002).

# References

[1] M. L. Wilkins, Calculation of elastic-plastic flow, Tech. rep., California Univ Livermore Radiation Lab (1963).

[2] S. L. Gavrilyuk, N. Favrie, R. Saurel, Modelling wave dynamics of compressible elastic materials, Journal of computational physics 227 (5) (2008) 2941–2969.

[3] J.-B. Cheng, E. F. Toro, S. Jiang, M. Yu, W. Tang, A high-order cell-centered Lagrangian scheme for one-dimensional elastic–plastic problems, Computers & Fluids 122 (2015) 136–152.

[4] J. Cheng, Harten-Lax-van Leer-contact (HLLC) approximation Riemann solver with elastic waves for one-dimensional elastic-plastic problems, Applied Mathematics and Mechanics 37 (11) (2016) 1517–1538.

[5] L. Liu, J.-b. Cheng, A multi-material hllc riemann solver with both elastic and plastic waves for 1d elastic-plastic flows.

[6] X. Garaizar, Solution of a Riemann problem for elasticity, Journal of elasticity 26 (1) (1991) 43–63.

[7] G. H. Miller, An iterative riemann solver for systems of hyperbolic conservation laws, with application to hyperelastic solid mechanics, Journal of Computational Physics 193 (1) (2004) 198–225.

[8] S. Gao, T. Liu, 1d exact elastic-perfectly plastic solid Riemann solver and its multi-material application, Advances in Applied Mathematics and Mechanics 9 (3) (2017) 621–650.

[9] S. Gao, T. Liu, C. Yao, A complete list of exact solutions for one-dimensional elastic-perfectly plastic solid riemann problem without vacuum, Communications in Nonlinear Science and Numerical Simulation 63 (2018) 205–227.

[10] P.-H. Maire, R. Abgrall, J. Breil, R. LoubèRe, B. Rebourcet, A nominally second-order cell-centered Lagrangian scheme for simulating elastic–plastic flows on two-dimensional unstructured grids, Journal of Computational Physics 235 (2013) 626–665.